Photoelectrochemical performance of TiO_2-ZnO nanocrystalline composite thin films

D. B. Shinde[1], Y. A. Pawar[1], A. P. Nikum[1], P. N. Bhosale[2], R. K. Mane[3]
[1]S.P.K. Mahavidyalaya, Sawantwadi-416510, Dist. Sindhudurg, India
[2]Materials Research Laboratory, Department of Chemistry, Shivaji University, Kolhapur-416004, India
[3]Smt. K.R.P.Kanya Mahavidyalaya, Islampur-415409, Dist.-Sangli, India

Abstract: High density TiO_2 nanorods were hydrothermally deposited on transparent conducting oxide substrate followed by deposition of ZnO nanorods by simple chemical reflux method at low temperature (140^O). The structural, morphological, compositional and electrochemical properties are investigated by detailed XRD, SEM, TEM, EDAX, XPS and photoelectrochemical studies. The compact and well aligned TiO_2-ZnO composite nanorods were grown on the overall substrate surface showed photoelectrochemical (PEC) performance η = 3.8 %.

IndexTerms *- Nanocomposite architecture, Nanorods, Photoconversion efficiency.*

1. INTRODUCTION

There has been increasing interest during the last few decades to find out an alternative cost effective renewable energy sources to fulfill the future energy needs of mankind. In this respect synthesis of tailored morphological mixed transitional metal oxide (TMO) semiconducting thin films because of their widespread applications in optoelectronic fields of science and technology leading to drastic cut in the production cost of semiconducting devices [1-2]. Recently, considerable interest has focused on synthesis of nanocomposite films and powders such as TiO_2-ZnO, TiO_2-SiO_2, TiO_2-WO_3, and TiO_2-CdSe which have been considered as effective semiconductors [3-5]. Many attempts have been made to synthesize coupled bicomponent ZnO-TiO_2 nanocomposite by a physical or chemical process with two aims, (i) extending the light adsorption spectrum and improving the conversion efficiency and (ii) suppressing the recombination of photogenerated electron/hole pairs. This nanocomposite may increase the PEC conversion efficiency by increasing the charge separation and extending the photoresponding range [6-8].

In this context, there has been considerable effort made toward the investigation of TiO_2-ZnO nanocomposite, however, to the best of our knowledge, little attention has been paid to investigate the PEC performance of coupled ZnO-TiO_2 nanorod structures. Therefore considering the above fact and literature survey, in the present attempt we synthesize and studied the PEC performance of TiO_2-ZnO nanocomposite thin films.

2. METHOD AND MATERIALS

Fluorine doped tin oxide (FTO) coated glass substrates was used as a conducting substrate support for deposition. All chemical reagents used were analytical reagent (AR) grade. Zinc acetate dihydrate ($Zn(CH_3COO)_2 \cdot 2H_2O$), hexamethylenetetraamine (HMTA) ($(CH_2)_6N_4$) used as the Zn precursor. Titanium tetraisopropoxide (TTIP) (99.98% Spectrochem, India), Concentrated hydrochloric acid (35.4% Thomas Baker) used as the Ti precursor. The aqueous solution was prepared using double distilled water.

3. THIN FILM SYNTHESIS

In a typical TiO_2 thin film synthesis 0.5 ml titanium tetra isopropoxide (TTIP) was added in aqueous solution containing 1:1 HCl and stirred vigerously to obtained clear and transparent solution. The resultant solution was added into teflon lined stainless steel autoclave. The conducting FTO glass substrate is immersed into autoclave and autoclave was sealed and placed in an oven at 140ºC for 5 hr followed by natural cooling to room temperature. The substrate was removed from autoclave, cooled at room temperature and rinsed thoroughly using double distilled water. The 50 ml of zinc acetate dihydrate and 50 ml of HMTA solutions were prepared in double distilled water. These two solutions were mixed and stirred for 10 minutes. The TiO_2 deposited FTO substrate were dipped in the solution and refluxed at 77 ±2 ºC for 5 hr to deposit pure ZnO thin films. Finally, the substrate washed with double distilled water, dried at room temperature and used for further characterization without post annealing treatment.

4.1. STRUCTURAL STUDY

Fig.1 shows XRD pattern of TiO_2-ZnO thin film sample. The intense peak at 27.55^0 is the representative peak for (110) plane of rutile TiO_2. XRD patterns exhibited strong diffraction peaks at 27.55°, 36.79°and 55.40° indicating formation of pure hexagonal

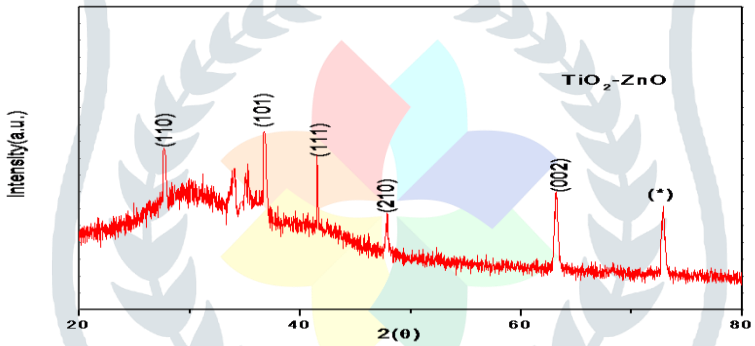

Fig.1 XRD pattern of TiO_2- ZnO thin film sample.

wurtzite phase ZnO and tetragonal rutile phase of TiO_2 material. All peaks are in good agreement with the standard JCPDS data (Card no. 80-0078 and Card No. 00 001-0562) [9-10]. The other peaks shown by asterisks are due to the FTO substrate marked by *. Average crystallite size of TiO_2-ZnO samples were calculated by using Scherrer's formula shown in equation (1).

$$D = \frac{0.94\,\lambda}{\beta \cos\theta} \qquad (1)$$

Where 'D' is the crystallite size, 'θ' is peak position of X-ray used, 'β' is full width at half maxima FWHM and '$\boldsymbol{\lambda}$' is wavelength of X-ray used (0.154 nm). The calculated crystallite size of TiO_2-ZnO for (110) plane is found to be 30.47 nm.

4.2. MORPHOLOGICAL STUDY

Fig.2 (a, b) shows SEM images of the composite TiO_2-ZnO nanorods. It shows smooth, completely grown and regularly arranged nanorods at the bottom layer with irregularly arranged nanorod flowers on their top surface.

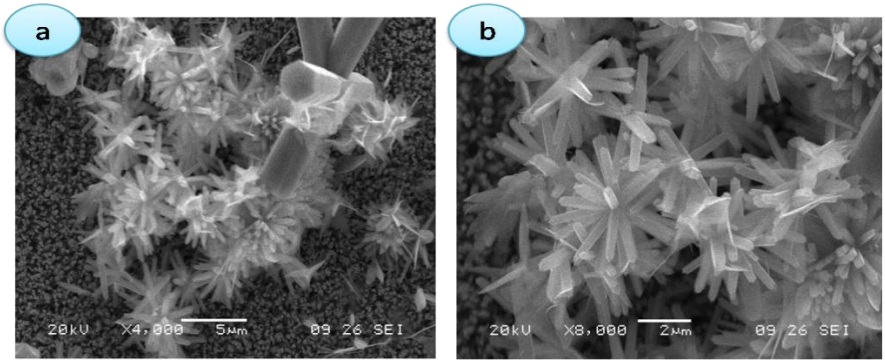

Fig.2 (a, b) SEM images of TiO_2- ZnO thin film sample.

Fig.3 (a) shows the TEM image focused on a single nanorod. A nanorod is having 100 to 150 nm diameter and a tetragonal architecture with a smooth surface. The sharp SAED pattern shown in Fig.3 (b), indicate nanorod is single crystalline. The Fig.3 (c) shows the HRTEM pattern of TiO_2-ZnO sample with the lattice spacing 0.344 nm corresponding to the d-spacing of the (110) plane of rutile TiO_2 and 0.24nm corresponds to (002) plane of wurtzite ZnO [11-13].

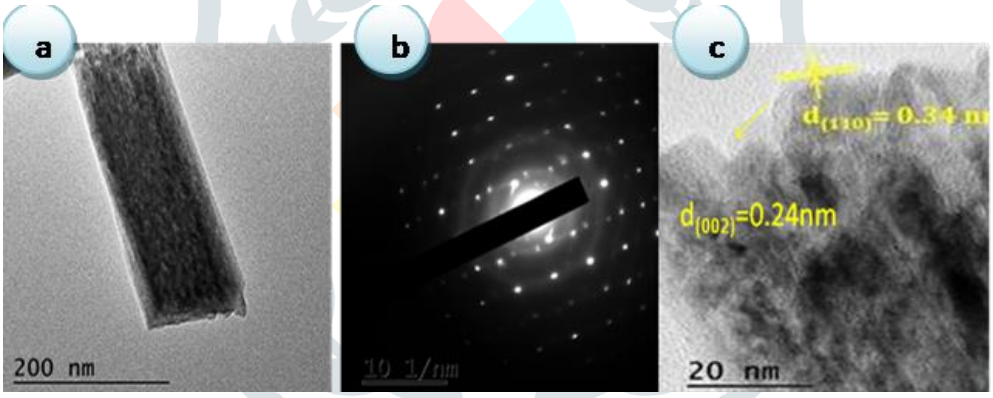

Fig.3 (a) shows TEM image**, (b)** SAED pattern and **(c)** HRTEM image of TiO_2- ZnO sample.

4.3. COMPOSITIONAL ANALYSIS

Fig.4 shows an EDS pattern obtained for TiO_2-ZnO sample. There is no trace of any other impurities could be seen within the detection limit of the EDS. The corresponding EDS results confirm the formation TiO_2-ZnO thin films.

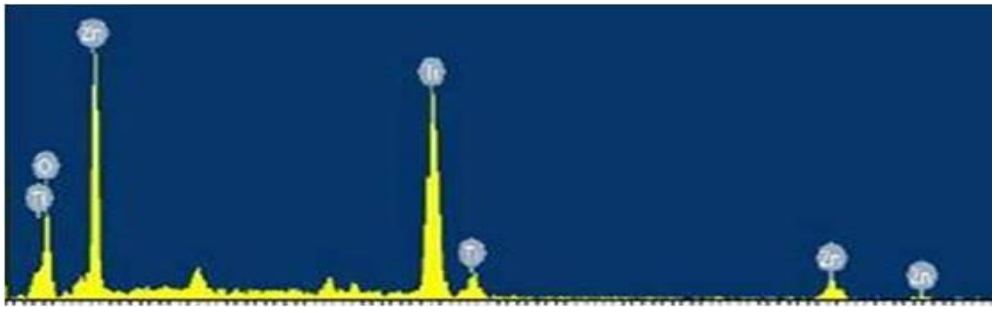

Fig.4 Shows Energy Dispersive X-ray (EDX) spectrum of TiO_2- ZnO thin film.

The XPS analysis of TiO2-ZnO thin films was performed to identify the composition and valence state of elements. The survey spectrum of TiO_2-ZnO sample is presented in Fig.5. It shows presence of Zn, Ti, O and a small amount of adventitious carbon. The carbon peak is attributed to the residual carbon from XPS instrument itself. The peak at binding energy 284.87 eV corresponds to amorphous carbon. The peaks at 1021.25 eV and 1044.36 eV assigned to the electronic states of $Zn2P_{3/2}$ and $Zn2P_{1/2}$, respectively. It indicates that Zn ions exist in +2 oxidation state [14]. Figure consists of the distinct Ti /2p1/2 and Ti /2p3/2 signals that are located at 464.4 and 458.6 eV respectively. The spin orbital splitting between these peaks is 5.8 eV which is comparable with 5.74 eV reported value, indicates Ti^{4+}oxidation state [15].

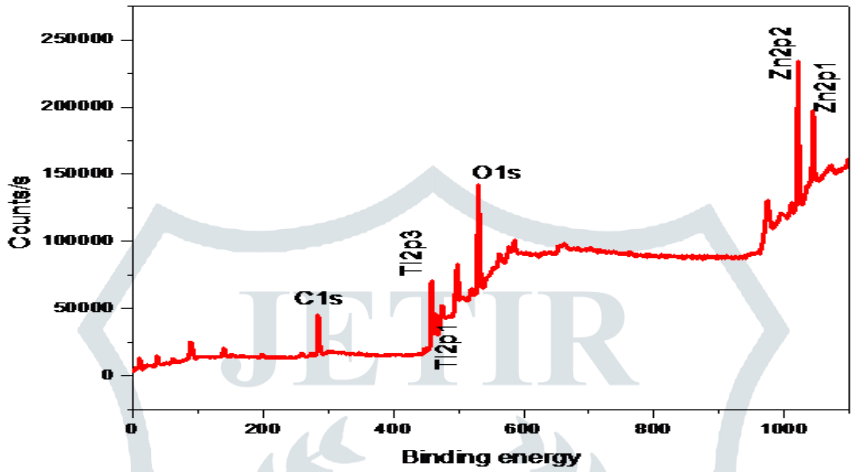

Fig. 5 Experimental survey spectrum of TiO_2-ZnO sample.

4.4. PHOTOELECTROCHEMICAL PROPERTY

The metal oxide semiconductors can absorb large amount of light radiation to form photogenerated electron–hole pairs. The photogenerated electrons can transport directly through crystallites and compact layers to the conducting substrates with minimum loss. This photo generated electrons travel through the external load and completes the circuit by entering back through the counter electrode [16].

The J-V characteristic curve of TiO_2-ZnO thin films under UV illumination in light and dark is shown in Fig. 6 (a). The two electrode system was fabricated to study PEC property as,

Glass - FTO / TiO_2-ZnO / 0.1 M Na_2SO_4 / Graphite

The PEC parameters such as fill factor (FF) and PEC efficiency (η%) was calculated by Equation (2) and (3) given as,

$$FF = \frac{Jmax\ Vmax}{Jsc\ Voc} \qquad (2)$$

$$\eta\ \% = \frac{Jsc\ Voc}{Pin} \times FF \times 100 \qquad (3)$$

where, '*Vmax'* is maximum voltage, '*Jmax'* is maximum current density, '*Jsc'* is short circuit current density, '*Voc'* is open circuit voltage *and 'Pin'* is intensity of incident light. The photocurrent could not be detected unless nanostructured TiO_2-ZnO photoanode illumines with UV light. When the nanostructure photoanode were illuminated under UV light, photovoltage were rises rapidly to a constant value causes shift in the fourth quadrant indicating the generation of electricity, which are typical solar cell characteristics [17]. These PEC parameters TiO_2-ZnO sample is summarized in Table.

V_{oc} (mV)	V_{max} (mV)	J_{sc} (mA/cm^2)	J_{max} (mA/cm^2)	FF	η %
747	414	0.654	0.463	0.39	3.8

The PEC measurement showed photoconversion efficiency η = 3.8%. An open circuit voltage-decay measurement was conducted to investigate recombination kinetics of nanostructure and is shown in Fig. 6 (b). Adopting the technique reported by Zaban et al. open circuit voltage-decay measurements are performed. It showed that the response of these electrodes to UV illumination was very prompt [18].

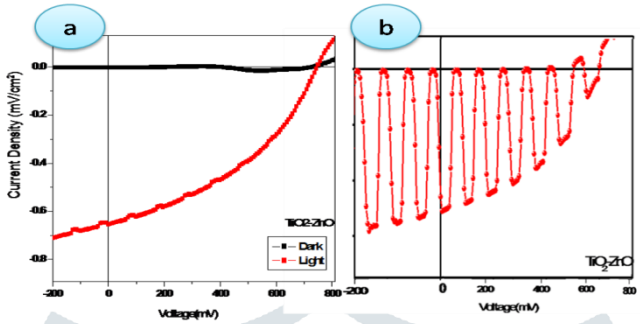

Fig. 6 (a) J-V characteristic curve and (b) chopping curve of TiO_2- ZnO sample.

5. CONCLUSIONS

We successfully deposited composite TiO_2-ZnO thin films with nanorod morphology. The XRD, SEM, TEM and EDS analysis evidenced the structural differences and the high degree of crystallinity of these materials. The PEC measurements showed that TiO_2-ZnO composite thin films showed 3.8% conversion efficiency. The PEC performance has been attributed due to stronger light scattering effects, faster electron transportation and electrolyte diffusion in densely and uniformly covered TiO_2-ZnO nanorod sample.

REFERENCES

1. P. K. Santra and P. V. Kamat, (2012), J. Am. Chem. Soc., 134, (5) 2508-2511.
2. R. Bel-Hadj-Tahar, A. B. Mohamed, (2014), N. J. Glass and Ceramics, (4), 55-65.
3. R. A. Naphade, M. Tathavadekar, J. P. Jog, S. Agarkar and S. Ogale, (2014), J. Mater. Chem. A, (2), 975-984.
4. E. Guo and L. Yin, (2015), J. Phys. Chem., 17, 563-574.
5. A. I. Ali, A. H. Ammar, A. A. Moez, (2015), J. Superlat. and Microstr. 65, 285–298.
6. Y. S. Kobayashi, H. Narita, T. Kanehira, K. Sonezaki, S. Kubota, Y. Terasaka, S. Iwasaki, (2010), Photochem. Photobiol., 86, 964 - 971.
7. Z. He, J. Liu, J. Miao, B. Liu, T. Thatt, (2014) J Mater Chem C (2), 1381-1385.
8. S. S. Mali, C. A. Betty, P.N. Bhosale, P.S. Patil (2011) J Cryst.Eng.Comm.13,6349-6351.
9. C.W. Kim, U. Pal, S. Park, Y.H. Kim, J. Kim, Y.S. Kang, (2012) RSC Adv. 2, 11969.
10. M. Salari, S. H. Aboutalebi, A. Aghassi, P. Wagner, A.J. Mozer, G.G. Wallace, (2015) Phys. Chem.17, 5642.
11. J. Li, W. Wan, H. Zhou, J. Li and, D. Xu, (2012) Chem. Commun., 48, 389-393.

12. D. B. Shinde, S. K. Jagadale, R. K. Mane, R. M. Mane, S.S. Mali, C. K. Hong and P. N. Bhosale, (2015), J. Nanomed. Nanotech. S7:004, 2157-7439.
13. P. S. Shinde, P. S. Patil, P. N. Bhosale, C. H. Bhosale, (2008), J. Appl. Catal. B: Env., 89, 288-293.
14. G. Poongodi, P. Anandan, R. M. Kumar, R. Jayavel, (2015), J. Pectrochimica Acta Part A. Mol. and Biomol. Spectro., 148, 237–243.
15. P. B. Patil, S. S. Mali, V.V. Kondalkar, N. B. Pawar, K. V. Khot, C. K. Hong, P. S. Patil, P. N. Bhosale, (2014), RSC Adv. 4, 47278.
16. D. B. Shinde, P. N. Bhosale and R. K. Mane (2018) J. AIIRJ, Vol.-V, III, 32-36.
17. S. Hoang, S. Guo, N. T. Hahn, A. J. Bard, C. B. Mullins, Nano Lett., (2011), 12, 26–32.
18. J. R. Jennings, A. Ghicov, L. M. Peter, P. Schmuki and A. B. Walker, J. Am. Chem. Soc., (2008), 130, 13364–13372.